Journal Pre-proof

Bisphenol-S and Bisphenol-F alter mouse pancreatic β-cell ion channel expression and activity and insulin release through an estrogen receptor ERβ mediated pathway

Laura Marroqui, Juan Martinez-Pinna, Manuel Castellano-Muñoz, Reinaldo S. dos Santos, Regla M. Medina-Gali, Sergi Soriano, Ivan Quesada, Jan-Ake Gustafsson, José A. Encinar, Angel Nadal

PII: S0045-6535(20)33248-3

DOI: https://doi.org/10.1016/j.chemosphere.2020.129051

Reference: CHEM 129051

To appear in: *ECSN*

Received Date: 1 October 2020

Revised Date: 17 November 2020

Accepted Date: 18 November 2020

Please cite this article as: Marroqui, L., Martinez-Pinna, J., Castellano-Muñoz, M., dos Santos, R.S., Medina-Gali, R.M., Soriano, S., Quesada, I., Gustafsson, J.-A., Encinar, J.A., Nadal, A., Bisphenol-S and Bisphenol-F alter mouse pancreatic β-cell ion channel expression and activity and insulin release through an estrogen receptor ERβ mediated pathway, *Chemosphere*, https://doi.org/10.1016/j.chemosphere.2020.129051.

This is a PDF file of an article that has undergone enhancements after acceptance, such as the addition of a cover page and metadata, and formatting for readability, but it is not yet the definitive version of record. This version will undergo additional copyediting, typesetting and review before it is published in its final form, but we are providing this version to give early visibility of the article. Please note that, during the production process, errors may be discovered which could affect the content, and all legal disclaimers that apply to the journal pertain.

© 2020 Elsevier Ltd. All rights reserved.

Journal Pre-proof

Credit Author Statement

LM: Conceptualization, Supervision, Investigation, Formal Analysis, Visualization, Writing - Review & Editing **JMP**: Conceptualization, Investigation, Formal Analysis, Visualization, Writing - Review & Editing **MCM**: Investigation, Formal Analysis, Visualization, Writing - Review & Editing **RSdS**: Investigation, Formal Analysis, Writing - Review & Editing **RMMG**: Investigation, Formal Analysis, Writing - Review & Editing **SS**: Investigation, Formal Analysis, Visualization, Writing - Review & Editing **IQ**: Visualization, Resources, Funding Acquisition, Writing - Review & Editing **J-AG**: Resources, Writing - Review & Editing **JAE**: Conceptualization, Investigation, Visualization, Resources, Funding Acquisition, Writing - Review & Editing **AN**: Conceptualization, Supervision, Visualization, Resources, Funding Acquisition, Writing - Original Draft, Project Administration. All authors have given approval to the final version of the manuscript.

Journal Pre-proof

Journal Pre-proof

Bisphenol-S and Bisphenol-F alter mouse pancreatic β-cell ion channel expression and activity and insulin release through an estrogen receptor ERβ mediated pathway

Laura Marroqui[1,2], Juan Martinez-Pinna[1,3], Manuel Castellano-Muñoz[2], Reinaldo S. dos Santos[1,2], Regla M. Medina-Gali[1,2], Sergi Soriano[1,3], Ivan Quesada[1,2], Jan-Ake Gustafsson[4,5], José A. Encinar[1] and Angel Nadal[1,2,*].

1. Instituto de Investigación, Desarrollo e Innovación en Biotecnología Sanitaria de Elche (IDiBE), Universitas Miguel Hernández, Elche, Spain.

2. Centro de Investigación Biomédica en Red de Diabetes y Enfermedades Metabólicas Asociadas (CIBERDEM), Spain.

3. Departamento de Fisiología, Genética y Microbiología, Universidad de Alicante, Alicante, Spain.

4. Department of Cell Biology and Biochemistry, Center for Nuclear Receptors and Cell Signaling, University of Houston, Houston, TX, USA.

5. Department of Biosciences and Nutrition, Karolinska Institutet, Huddinge, Sweden

Correspondence to: Prof. Angel Nadal, IDiBE, Miguel Hernandez University, 03202-Elche, Alicante, Spain. Phone: +34 965222002, email: nadal@umh.es

KEYWORDS: Bisphenol, Islet of Langerhans, Endocrine Disrupting Chemicals, Estrogen Receptors, Molecular Dynamics Simulation

Journal Pre-proof

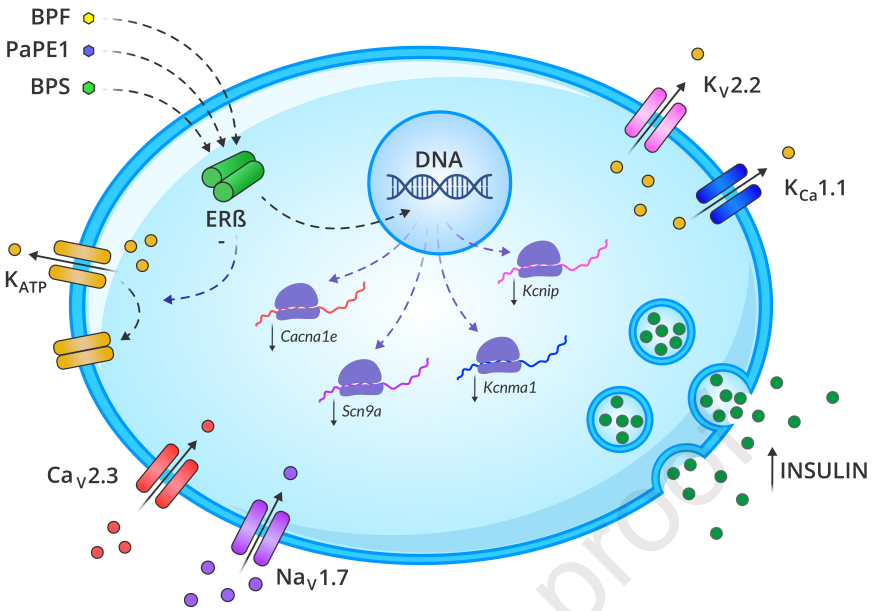

Journal Pre-proof

Journal Pre-proof

ABSTRACT

Bisphenol-S (BPS) and Bisphenol-F (BPF) are current Bisphenol-A (BPA) substitutes. Here we used pancreatic β-cells from wild type (WT) and estrogen receptor β (ERβ) knockout (BERKO) mice to investigate the effects of BPS and BPF on insulin secretion, and the expression and activity of ion channels involved in β-cell function. BPS or BPF rapidly increased insulin release and diminished ATP-sensitive K^+ (K_{ATP}) channel activity. Similarly, 48 h treatment with BPS or BPF enhanced insulin release and decreased the expression of several ion channel subunits in β-cells from WT mice, yet no effects were observed in cells from BERKO mice. PaPE-1, a ligand designed to preferentially trigger extranuclear-initiated ER pathways, mimicked the effects of bisphenols, suggesting the involvement of extranuclear-initiated ERβ pathways. Molecular dynamics simulations indicated differences in ERβ ligand-binding domain dimer stabilization and solvation free energy among different bisphenols and PaPE-1. Our data suggest a mode of action involving ERβ whose activation alters three key cellular events in β-cell, namely ion channel expression and activity, and insulin release. These results may help to improve the hazard identification of bisphenols.

Journal Pre-proof

1. INTRODUCTION

The relationship between BPA exposure and hormone related diseases (Gore et al., 2015) has raised consumers concern. Consequently, BPA has been progressively substituted by other bisphenol analogs. Among the nearly 15 bisphenol analogs, BPS and BPF are widely consumed and commercialized (Rochester and Bolden, 2015), being the major bisphenol contaminants in indoor dust along with BPA (Liao et al., 2012b). Similar to BPA, the detection frequencies of BPS and BPF were approximately 80% in urine samples collected from the general United States population and several Asian countries (Liao et al., 2012a; Ye et al., 2015). In the United States population, the detection frequency of BPS in urine has increased between 2000 and 2014 while that of BPA trends to decrease since 2010. BPA had a frequency and geometric mean concentrations of 74−99% and 0.36−2.07 μg/L, followed by BPF 42−88%, 0.15−0.54 μg/L and BPS, 19−74%, < 0.1−0.25 μg/L (Ye et al., 2015). BPA has a tolerable daily intake (TDI) determined by the European Food Safety Authority in 2015 of 4 μg/kg-day and in 2017 it was identified by the European Chemical Agency as a substance of very high concern due to its endocrine disrupting properties (Beausoleil et al., 2018). Of note, TDIs for other bisphenols do not yet exist.

BPA has been considered a risk factor in the etiology of type 2 diabetes (T2D) (Alonso-Magdalena et al., 2006; Ropero et al., 2008; Nadal et al., 2009; Batista et al., 2012). Epidemiological and prospective studies associated BPA exposure with alterations in glucose homeostasis or T2D incidence, independently of obesity or other traditional factors (Lang et al., 2008; Shankar and Teppala, 2011; Beydoun et al., 2014; Ranciere et al., 2019). Recent epidemiological data associated BPS urine levels with T2D development in a case-cohort study (Ranciere et al., 2019) and a case-control study (Duan et al., 2018). BPF has been recently

39 associated with abdominal obesity in children (Jacobson et al., 2019), but association with T2D
40 is still unclear.

41 T2D occurs due to a progressive loss of sufficient β-cell insulin secretion frequently on the
42 background of insulin resistance (American Diabetes, 2018). The use of animal and cellular
43 models indicated a link between BPA exposure and diabetes development (Nadal et al., 2009;
44 Alonso-Magdalena et al., 2011; Le Magueresse-Battistoni et al., 2018). Adult male mice exposed
45 to environmentally relevant doses of BPA presented insulin resistance and hyperinsulinemia in
46 fed state (Alonso-Magdalena et al., 2006; Batista et al., 2012). Furthermore, BPA directly
47 affected β-cell function (Quesada et al., 2002; Alonso-Magdalena et al., 2008; Soriano et al.,
48 2012; Martinez-Pinna et al., 2019). Pancreatic β-cells are excitable cells and, therefore, their
49 electrical activity rules stimulus-secretion coupling. A primary event in the mechanism of insulin
50 release is the inhibition of the ATP-sensitive K^+ (K_{ATP}) channels, which control β-cell resting
51 membrane potential. This inhibition leads to a typical electrical activity pattern consisting of
52 bursts of action potentials produced by the opening of voltage-gated, Ca^{2+}, Na^+ and K^+ channels,
53 as well as a rise in intracellular Ca^{2+}, which culminates in insulin exocytosis (Rorsman and
54 Ashcroft, 2018). Changes in the expression and/or function of these ion channels result in altered
55 insulin secretion and constitute a serious risk factor for T2D (Hiriart et al., 2014; Jacobson and
56 Shyng, 2020).

57 Even though BPA may act through different modes of action, it is considered a xenoestrogen
58 able to bind to ERβ and ERα (Wetherill et al., 2007). Both ERs exert their actions through
59 nuclear- and extranuclear-initiated pathways. The nuclear-initiated pathway consists of the direct
60 binding of the ligand bound-ERs to estrogen response elements, which are located in the
61 regulatory regions of ER target genes (Smith and O'Malley, 2004; Heldring et al., 2007).

Transcriptional regulation also occurs through tethering of ERs to DNA-bound transcription factors AP-1 and Sp-1 (Ascenzi et al., 2006). Conversely, extranuclear-initiated pathways involve the activation of intracellular signaling cascades that will lead to different effects, including transcriptional regulation (Levin and Hammes, 2016). Although the role of extranuclear-initiated events triggered by environmental estrogens remains poorly understood, rodent models and human studies indicate that this pathway may be important to initiate effects at low doses (Alonso-Magdalena et al., 2008; Vinas and Watson, 2013; Acconcia et al., 2015; Nadal et al., 2018).

In β-cells, nanomolar (1-10nM) concentrations of 17β-estradiol (E2) and BPA rapidly (within 10 minutes) inhibit K_{ATP} channels and enhance glucose-stimulated insulin secretion (GSIS) in an ERβ-dependent mechanism (Soriano et al., 2009; Soriano et al., 2012). Longer exposures to BPA (48 h) regulate gene expression of Ca^{2+}, Na^{+} and K^{+} channels, altering electrical activity, Ca^{2+} signaling, and insulin release (Villar-Pazos et al., 2017; Martinez-Pinna et al., 2019). In addition, BPA exposure for 48 h also increases β-cell division in vivo as well as in primary cells. These effects are mimicked by ERβ agonists and abolished in cells from ERβ knockout mice (BERKO), which do not express ERβ in β-cells, suggesting that ERβ activation is necessary for BPA effects in pancreatic β-cells (Boronat-Belda et al., 2020).

Here we studied BPS and BPF effects on insulin release, and ion channel expression and activity in β-cells from wild type (WT) and BERKO mice. Because evidence suggested an important role of ERβ via an extranuclear-initiated pathway, we compared effects elicited by bisphenols with those induced by Pathway Preferential Estrogen-1 (PaPE-1), a compound that binds to ERs and acts preferentially through extranuclear-initiated pathways (Madak-Erdogan et al., 2016). Additionally, we performed molecular docking and dynamic simulations of bisphenols, PaPE-1

and E2 bound to the ERβ ligand-binding domain (LDB) to evaluate the consistencies and variances among these ligands at the molecular level.

2. Materials and methods

2.1 Chemical substances

Bisphenol-A was obtained from MP Biomedicals (Cat No 155118; Santa Ana, CA, USA). BPS (Cat No 103039), BPF (Cat No 51453), PaPE-1 (Cat No SML1876), and collagenase (Cat No C9263) were obtained from Sigma-Aldrich (Barcelona, Spain). Bisphenols and PaPE-1 were weekly prepared by dissolution in DMSO (used as vehicle).

2.2 Animals, islet culture and dispersed islet cells

All adult male mice were kept under standard housing conditions (12 h light/dark cycle, food *ad libitum*). BERKO mice were generated as described previously (Krege et al., 1998) and supplied by Jan-Ake Gustafsson's laboratory. Both WT littermates and BERKO mice were acquired from the same supplier and colony. Mice were sacrificed and islets were isolated as previously described (Nadal and Soria, 1997). For patch-clamp experiments, islets were dispersed into single cells and plated on glass coverslips as described before (Valdeolmillos et al., 1992). Cells were kept at 37 °C in a humidified atmosphere of 95% O_2 and 5% CO_2 and used within 48 h of culture. Experimental procedures were performed according to the Spanish Royal Decree 1201/2005 and the European Community Council directive 2010/63/EU. The ethical committee of Miguel Hernandez University reviewed and approved the methods used herein (approvals ID: UMH-IB-AN-01–14 and UMH-IB-AN-02-14).

2.3 Glucose-stimulated insulin secretion (GSIS)

GSIS was performed in islets as previously described (Santin et al., 2016) with slight changes. Briefly, islets were preincubated for 1 h in glucose-free Krebs-Ringer solution. Afterward, islets were sequentially stimulated with 2.8, 8.3, and 16.7 mM glucose for 1 h either in the presence or absence of treatments (as described in Figure 1). Insulin release and insulin content were measured in islet-free supernatants and acid ethanol-extracted islets lysates, respectively, using a mouse insulin ELISA kit (Mercodia, Uppsala, Sweden).

2.3 Patch-clamp recordings

K_{ATP} channel activity was recorded using standard patch-clamp recording procedures from isolated β-cells as described previously (Valdeolmillos et al., 1992; Vettorazzi et al., 2016). Around 80-90% of the single cells were identified as β-cells. Currents were recorded using an Axopatch 200B patch-clamp amplifier (Axon Instruments Co. CA, USA). Patch pipettes were pulled from borosilicate capillaries (Sutter Instruments Co. CA, USA) using a flaming/brown micropipette puller P-97 (Sutter Instruments Co. CA, USA) with resistance between 3–5 MΩ when filled with the pipette solutions as specified below. Bath solution contained (in mM): 5 KCl, 135 NaCl, 2.5 CaCl2, 10 Hepes and 1.1 $MgCl_2$ (pH 7.4) and supplemented with glucose as indicated. The pipette solution contained (in mM): 140 KCl, 1 $MgCl_2$, 10 Hepes and 1 EGTA (pH 7.2). The pipette potential was held at 0 mV throughout recording. K_{ATP} channel activity was quantified by digitizing 60 s sections of the current record, filtered at 1 kHz, sampled at 10 kHz by a Digidata 1322A (Axon Instruments Co. CA, USA), and calculating the mean open probability of the channel (NP_o) during the sweep. Channel activity was defined as the product of

130 *N*, the number of functional channels, and P_o, the open-state probability. *Po* was determined by
131 dividing the total time channels spent in the open state by the total sample time.
132 For the patch-clamp recordings of voltage-gated Ca^{2+} currents, the whole-cell patch-clamp
133 configuration was used as described previously (Villar-Pazos et al., 2017). Pancreatic β-cells
134 were identified by size (>5 pF) and the corresponding steady-state inactivation properties of the
135 tetrodotoxin (TTX)-sensitive Na^+ current. Data were obtained using an Axopatch 200B patch-
136 clamp amplifier (Axon Instruments Co. CA, USA). Patch pipettes were pulled from borosilicate
137 capillaries (Sutter Instruments Co. CA, USA) using a flaming/brown micropipette puller P-97
138 (Sutter Instruments Co. CA, USA) and heat polished at the tip using an MF-830 microforge
139 (Narishige, Japan). The bath solution contained 118 mM NaCl, 20 mM TEA-Cl, 5.6 mM KCl,
140 2.6 mM CaCl2, 1.2 mM MgCl2, 5 mM HEPES and 5 mM glucose (pH 7.4 with NaOH). The
141 pipette solution consisted of 130 mM CsCl, 1 mM CaCl2, 1 mM MgCl2, 10 mM EGTA, 3 mM
142 MgATP and 10 mM HEPES (pH 7.2 with CsOH). After filling the pipette with the pipette
143 solution, the pipette resistance was 3–5 MΩ. A tight seal (>1 GΩ) was established between the β-
144 cell membrane and the tip of the pipette by gentle suction. The series resistance of the pipette
145 usually increased to 6–15 MΩ after moving to whole-cell. Series resistance compensation was
146 used (up to 70%) for keeping the voltage error below 5 mV during current flow. Voltage-gated
147 Ca^{2+} currents were compensated for capacitive transients and linear leak using a -P/4 protocol.
148 Data were filtered (2 kHz) and digitized (10 kHz) using a Digidata 1322 A (Axon Instruments
149 Co. CA, USA) and stored in a computer for subsequent analysis using commercial software
150 (pClamp9, Axon Instruments Co. CA, USA). Experiments were carried out at 32–34 °C.
151
152 *2.4 Quantitative real-time PCR*

Journal Pre-proof

Total RNA was isolated using the RNeasy Micro Kit (Qiagen) and reverse-transcribed using the High Capacity cDNA Reverse Transcription Kit (Applied Biosystems). Quantitative PCR was performed using the CFX96 Real Time System (Bio-Rad, Hercules, CA) as described previously (Villar-Pazos et al., 2017). *Hprt* was used as housekeeping gene. The CFX Manager Version 1.6 (Bio-Rad) was used to analyse the values, which were expressed as relative expression ($2^{-\Delta\Delta Ct}$). The primers used herein have been previously described (Martinez-Pinna et al., 2019).

2.5 Molecular docking and dynamics simulations

Because ERα LBD and ERβ LBD have not been crystallized in mice while they have been resolved in rats, the latter was used for docking experiments. Crystallographic structure of the rat ERβ LBD in complex with pure antiestrogen ICI 164,384 [rERβ-ΔH12-LBD; UniProt code: Q62986, Protein Data Bank (PDB) code: 1HJ1] was used for molecular docking and long-time dynamic (1 μs) simulation purposes. The missing residues in the 1HJ1 structure (364-377) and the missing side chains (M242, K255, K269, E326, S363, S378, R379, K380 and K435) were reconstructed after generating a homology model at the Swiss-Model server (Biasini et al., 2014; Galiano et al., 2016). Structure of estradiol-bound rat ERβ LBD in complex with LXXLL motif from NCOA5 (rERβ-LBD; UniProt code: Q62986, PDB code: 2J7X) was used for molecular docking and short-time dynamic (100 ns) simulation purposes. The missing residues in the 2J7X structure (239-241 and 369-374) and the missing side chains (V237, M242, K255, E376, R374, K398, and K426) were reconstructed after generating a homology model at Swiss-Model server (Biasini et al., 2014; Galiano et al., 2016) using the 2J7X structure as a template. Molecular docking and dynamics simulations were carried out using YASARA structure v19.9.17 software as previously described (Encinar et al., 2015; Galiano et al., 2016; Ruiz-Torres et al., 2018). The

ligand-protein interactions have been detected with the Protein–Ligand Interaction Profiler (FLIP) algorithm (Salentin et al., 2015). Foldx 5.0-calculated (Delgado et al., 2019) was used for frequency distributions of intermolecular protein interaction energy for the subunits of the rERβ-ΔH12-LBD dimer in the presence of different ligands in each LBD cavity (Figure S5).

2.6 Data analysis

The GraphPad Prism 7.0 software (GraphPad Software, La Jolla, CA, USA) was used for statistical analyses. Data are presented as the mean ± SEM. Statistical analyses were performed using Student's t-test or one-way ANOVA. p values ≤ 0.05 were considered statistically significant.

3. Results

3.1 BPS and BPF affect insulin release

Previous data indicate that treatment with 1 nM BPA rapidly enhances insulin secretion in islets from mice and humans (Alonso-Magdalena et al., 2006; Soriano et al., 2012). To investigate whether BPS and BPF would have similar effects, we treated islets during 1 h with two concentrations of BPS and BPF (1 nM and 1 µM), and we measured insulin release in response to different glucose concentrations (2.8, 8.3 and 16.7 mM). Exposure to 1 nM and 1 µM BPS enhanced GSIS at stimulatory glucose concentration, mainly at 16.7 mM (**Figure 1A**). Regarding BPF, we observed a slight increase at 1 nM that was significant only in the presence of 16.7 mM glucose. BPF 1 µM, however, increased GSIS at both 8.3 and 16.7 mM glucose (**Figure 1B**). We used BPA as a positive control and 1 nM BPA increased GSIS, as expected

198 (**Figure S1A**). Of note, insulin content remained unchanged upon treatment with BPS, BPF, and
199 BPA (**Figure S1C-E**).
200 Longer BPA treatment (48 h) induced insulin hypersecretion in response to stimulatory glucose
201 concentrations (Alonso-Magdalena et al., 2008; Villar-Pazos et al., 2017). We then investigated
202 whether treatment with BPS or BPF during 48 h would also change GSIS. BPS at 1 nM and 1
203 µM enhanced insulin secretion in response to 8.3 mM glucose. However, when glucose
204 concentration was increased to 16.7 mM, BPS was effective at 1 nM but ineffective at 1 µM
205 (**Figure 1C**). When the same experiment in Figure 1C was performed with BPF, we only
206 observed a potentiation of insulin release at 1 µM at stimulatory glucose concentrations (**Figure**
207 **1D**), which indicated a more potent action of BPS compared to BPF. Treatment with BPA, BPS
208 or BPF did not modify insulin content (**Figure S1F-H**).
209
210 *3.2 BPS and BPF diminish K_{ATP} channel activity via ERβ*
211 We have previously demonstrated that acute BPA treatment potentiated GSIS after decreasing
212 K_{ATP} channel activity (Soriano et al., 2012). Moreover, BPA effects, which were not observed in
213 cells from BERKO mice, were reproduced by the endogenous ligand, 17β-estradiol (E2), as well
214 as the ERβ agonist diarylpropionitrile (DPN) (Soriano et al., 2009; Soriano et al., 2012). Acute
215 treatment with BPS induced a rapid increase in heart rate in response to catecholamines (Gao et
216 al., 2015). BPS also rapidly depressed left ventricular contraction and myocyte contractility
217 (Ferguson et al., 2019). In both cases, the ERβ antagonist PHTPP abolished BPS actions,
218 suggesting the involvement of ERβ (Gao et al., 2015; Ferguson et al., 2019).
219 To assess whether acute exposure to BPS or BPF would modulate K_{ATP} channel activity, we
220 performed patch-clamp recordings in the cell-attached mode in dispersed β-cells from WT and

BERKO mice (**Figure 2**). Treatment with 1 nM BPS during 10 minutes was enough to decrease K_{ATP} channel activity by 35% (**Figure 2A**,**B**), whereas no effects were observed in cells from BERKO mice (**Figure 2A**,**C**). A similar experiment was performed using 1 nM and 10 nM BPF. While 1 nM BPF did not modify K_{ATP} channel activity in β-cells from WT and BERKO (data not shown), 10 nM BPF decreased K_{ATP} channel activity in cells from WT (**Figure 2D**) but not in cells from BERKO mice (**Figure 2E**). These findings indicate that the rapid GSIS enhancement observed in **Figure 1A** may be a consequence of bisphenol-induced K_{ATP} channels closure.

The fact that this is a rapid action, occurring minutes upon treatment, indicates that low concentrations of bisphenols trigger a non-genomic action via an extranuclear-initiated pathway, likely by binding to ERβ. To test this hypothesis we used PaPE-1, a new ERα and ERβ ligand that acts preferentially through extranuclear-initiated pathways (Madak-Erdogan et al., 2016). Treatment with 1 µM PaPE-1 decreased K_{ATP} channel activity in cells from WT mice (**Figure 2F**) but had no effect in cells from BERKO mice (**Figure 2G**). Of note, 1 nM PaPE-1 did not change K_{ATP} channel activity (data not shown). These results emphasize that PaPE-1 triggers a rapid extranuclear-initiated pathway via ERβ in β-cells.

3.3 Bisphenols downregulate ion channel subunits gene expression

Stimulus-secretion coupling in β-cells depends on the electrical activity generated by ion channels. BPA treatment for 48 h decreased the mRNA expression of genes encoding Ca^{2+} (*Cacna1e*), K^+ (*Kcnma1* and *Kcnip1*) and Na^+ (*Scn9a*) channel subunits, which might explain, at least in part, the BPA-induced alteration in GSIS (Villar-Pazos et al., 2017; Martinez-Pinna et al., 2019). In Figure 3 A,E,I) we used BPA as a control to probe that in this preparation it decreased *Cacn1e*, *Kcnma1*, *Kcnip* and *Scn9* as already described (Villar-Pazos et al., 2017;

Martinez-Pinna et al., 2019). We found that BPS modulated *Cacna1e* mRNA expression in a non-monotonic dose response (NMDR)-dependent manner: exposure to 1 nM BPS reduced *Cacna1e* mRNA expression by 50%, while exposure to 100 nM and 1 µM did not significantly change *Cacna1e* expression (**Figure 3B**). This BPS-induced decrease in *Cacna1e* expression at 1 nM was associated to a reduction in Ca^{2+} currents in cells from WT (**Figure 4A,C,E**), but not in cells from BERKO (**Figure 4B,D,F**) mice. Of note, 100 nM and 1 µM BPS did not modify Ca^{2+} currents in cells from WT or BERKO mice (**Figure S2**). It is very likely that the decrease in Ca^{2+} currents induced by 1 nM BPS is a consequence of *Cacna1e* gene downregulation because both follow the same dose pattern. Regarding BPF, *Cacna1e* mRNA expression was not changed by treatment with 1 nM BPF for 48 h, but it was decreased upon exposure to 100 nM and 1 µM BPF (**Figure 3C**). Measurement of Ca^{2+} currents showed that only exposure to 1 µM BPF significantly decreased Ca^{2+} currents in cells from WT mice (**Figure 4G,I,K and Figure S3**), while no effects were observed in cells from BERKO mice (**Figure 4H,J,L and Figure S3**). Once again, we used PaPE-1 to study the possible involvement of an extranuclear-initiated pathway in the regulation of *Cacna1e* expression. Treatment with 1 µM PaPE-1 decreased *Cacna1e* expression (**Figure 3D**), which indicates that this gene can be regulated by a signaling pathway initiated outside the nucleus.

Like what we observed for *Cacna1e* expression, *Kcnma1* (**Figure 3E-H**), *Kcnip1* (**Figure 3I-L**), and *Scn9a* (**Figure 3M-P**) mRNA expression was downregulated by BPA, BPS, BPF and PaPE-1. BPS decreased *Kcnma1*, *Kcnip1*, and *Scn9a* at 1 nM in an NMDR manner, while BPF and PaPE-1 were effective at 1 µM (**Figure 3**).

As a negative control, we used 4,4'-(9-fluorenylidene)diphenol, BPFL (also named BHPF), which acts as an antiestrogen via ERs (Zhang et al., 2017; Keminer et al., 2019) but can also bind

267 to the androgen receptor (Zhang et al., 2017; Keminer et al., 2019). As expected, BPFL treatment
268 at different concentrations did not change ion channel gene expression or Ca^{2+} currents (**Figure**
269 **S4**).
270 Overall, these results demonstrate that BPS decreased the transcription of ion channel subunits at
271 concentrations as low as 1 nM, while BPF needed higher concentrations (100 nM and 1 µM) to
272 decrease the expression of the same genes. This effect was mimicked by PaPE-1, suggesting that
273 bisphenols may regulate gene expression via extranuclear ERs.
274 We previously used β-cells from BERKO mice as well as the ERβ ligand DPN to study the role
275 of ERβ on the regulation of ion channel subunit gene expression induced by BPA (Villar-Pazos
276 et al., 2017; Martinez-Pinna et al., 2019). To evaluate whether ERβ would also play a role in
277 BPS- and BPF-induced regulation of ion channel expression, we incubated islets from WT and
278 BERKO mice with 1 nM BPS or 1 µM BPF for 48 h. Similarly, to the results depicted in **Figure**
279 **3**, both 1 nM BPS and 1 µM BPF decreased *Cacna1e*, *Kcnma1* and *Scn9a* mRNA expression in
280 islets from WT mice (**Figure 5 A-C**). This decrease, however, was not observed in islets from
281 BERKO mice (**Figure 5 D-F**). Notably, 1 µM BPF increased *Cacna1e* expression in BERKO
282 mice, suggesting a role for receptors other than ERβ in the regulation of this gene.
283
284 *3.4 Molecular dynamics simulations of bisphenols bound to the rat ERβ LBD cavity.*
285 To investigate potential modifications in bisphenols and PaPE-1 binding to ERβ ligand binding
286 domain (LBD) that might help to, at least partially, explain the different biological activity of
287 bisphenols observed herein, we performed computational analyses of molecular docking and
288 dynamics simulations.

Despite the numerous studies using human ERα structures on molecular dynamics simulations (Celik et al., 2007; Fratev, 2015; Chen et al., 2016; Jereva et al., 2017; Li et al., 2018; Shtaiwi et al., 2018), the ERβ isoform has not yet been analyzed. Furthermore, ERα LBD and ERβ LBD have not been crystallized in mice, even though the resolved rat structure is well known. Because rat and mouse ERβ LBD sequences differ by only 3 amino acids, including two conservative mutations (**Figure S5A,B**), we chose to use rat structures in our analyses. A recent study using E2, BPA, BPS and BPAF indicated that the root mean square deviation (RMSD) values calculated from the heavy atoms of the ligands might be an important parameter to analyze ligand dynamics particularly implicated in nuclear-initiated events (Li et al., 2018). Therefore, to evaluate if our results fixed with a classic nuclear initiated event, we first studied molecular dynamics simulation of the transactivation helix (H12) closed rERβ-LBD. The natural ligand E2 showed no deviations from the starting configuration for over 100 ns (**Figure S6**), whereas deviations reached 2 Å in the presence of the Src coactivator peptide (**Figure S6**). Meanwhile, rearrangements in conformations are evident from the ligand heavy atom RMSDs in all three bisphenols. In addition, we observed that BPA and BPF showed rapid variations due to faster ring-flipping dynamics (**Figure S6A-C**), similarly to what has been previously shown (Li et al., 2018). The repositioning of H12 in the "mouse trap" conformation decisively influences the MM/PBSA solvation binding energy (Celik et al., 2007). We observed that the solvation binding energy for E2 and BPA was higher than that for BPS and BPF (**Figure S7**). Interestingly, BPS presented the lowest solvation binding energy value; thus, BPS should bind with lower affinity than BPF and BPA to this configuration, as experimentally demonstrated for the nuclear-initiated pathway (Molina-Molina et al., 2013). These results contrast with the order in biological activity described herein, where we find regulation of ion channel gene expression with at least 100-fold

lower concentrations of BPS than BPF. Therefore, a different mechanism to the classic nuclear-initiated event involved in the regulation of ion channel activity and gene expression in β-cells might be implicated in BPS and BPF effects.

We then sought to study differences and similarities among E2, BPA, BPS, BPF, and PaPE-1, using what we named rERβ-ΔH12-LBD (PDB code: 1HJ1; (Pike et al., 2001)) dimer complex, and performing long-time (1 μs) molecular dynamics simulations **(Figure 6A)**. In the rERβ-ΔH12-LBD complex, binding of the antiestrogen ICI 164,384 abrogates the association between H12 and the remainder of the LBD, and inhibits both of ER's transactivation functions (AF1 and AF2) (Pike et al., 2001). BPA does not stabilize ERα in a conformation that initiates nuclear events because BPA does not stabilize H12 (Delfosse et al., 2012). Then, simulating binding to rERβ-ΔH12-LBD dimer complex should be convenient to study extranuclear-initiated events.

Dimerization has been demonstrated to be necessary for ERs-mediated extranuclear responses (Razandi et al., 2004; Levin and Hammes, 2016). In our model, BPA, BPS and E2 showed similar frequency distributions of intermolecular protein interaction for both subunits of the dimers, whereas BPF and PaPE-1 presented lower frequency distribution (**Figure 6B**). This suggests a higher stability of the dimers with BPA, BPS and E2. Trajectories of the ligands docked in the LBD cavities (RMSD, Å) are similar except for PaPE-1 (**Figure 6C**), which left the open cavity of the LBD in both subunits after 700 ns (**Figure 6C**) and 840 ns (**Figure 6D**). For E2 and bisphenols, rearrangements rarely exceed 6 Å, indicating that the movement of the ligands into the cavity is limited, even when H12 is not closing the cavity. Notably, PaPE-1 MM/PBSA solvation binding free energy values, 60 kcal/mol (**Figure 6E**) and 65 kcal/mol (**Figure 6F**), indicate that this compound binds to the protein strongly than bisphenols and E2. On the other hand, bisphenols and E2 remain inside the cavity throughout the entire 1 μs

molecular dynamics simulation. We found very similar MM/PBSA solvation binding free energy values for E2 and BPA (around 55 kcal/mol), whereas BPS and BPF presented lower values (45 and 38 kcal/mol, respectively) (**Figure 6E,F**). The solvation binding energies correlated with the number of hydrogen bonds between the protein and the solvent (**Figure 6G)**. BPF presented the lowest solvation binding energy (**Figure 6E,F**) as well as the lowest number of hydrogen bonds (around 680 H-bonds, **Figure 6G**). These results indicate that BPF and PaPE-1 stabilize the ERβ-LBD dimer to a lesser extent than E2, BPA and BPS, which correlates with the lower biological activity observed for BPF and PaPE-1 in the present study. Therefore, we hypothesize that binding of bisphenols to the ERs induces a conformational change that favors an extranuclear-initiated action after dimerization of ERβ.

4. Discussion

In the present study we found that acute and long-term exposure of primary male mouse β-cells to BPS and BPF led to alterations in β-cell physiology across different levels of biological complexity, including K_{ATP} channel activity, Na^+, K^+ and Ca^{2+} channel subunits expression, and glucose-stimulated insulin release.

Although BPS and BPF have been used as alternatives to BPA, these chemicals may share some of the effects induced by BPA due to their similar structure (Malaise et al., 2020; Mustieles et al., 2020) or induce different effects to BPA (Kolla et al., 2018). We observed that, similarly to BPA, BPS and BPF enhanced GSIS either after acute treatment (1 h) or upon exposure for 48 h. The acute effect occurs at the two doses tested, 1 nM and 1 µM, and showed glucose dependence. Bisphenols had no effects at a non-stimulatory glucose concentration (3 mM), had a moderate effect at intermediate glucose concentration (8.3 mM), and had a stronger effect at high

glucose (16.7 mM). This potentiation was likely a consequence of the inhibition of K_{ATP} channels demonstrated using patch-clamp experiments in the cell-attached mode. In β-cells, K_{ATP} channels control the resting membrane potential. As a result of glucose metabolism, the rise in the ratio ATP/ADP blocks K_{ATP} channels and depolarizes the plasma membrane, thus initiating the electrical activity in burst of action potentials that culminates in insulin release. Here we show that BPS- and BPF-induced inhibition of K_{ATP} channels seems to potentiate the effect of glucose on insulin secretion, which leads to insulin hypersecretion.

The rapid BPA-induced potentiation of GSIS has been demonstrated in primary mouse and human β-cells (Soriano et al., 2012). In addition, oral BPA administration rapidly altered insulin and C-peptide levels in blood of adult individuals (Stahlhut et al., 2018; Hagobian et al., 2019). As in the present work BPS and BPF act akin to BPA in β-cells, an analogous effect on human cells might be expected. It is difficult to predict how this rapid action relates to the development of metabolic disorders. Pancreatic β-cells acutely exposed to bisphenols secrete more insulin than untreated cells, which may result in supraphysiological insulin signaling in some target tissues, such as adipose tissue.

Although human evidence are still scarce, BPS has been linked to T2D (Ranciere et al., 2019), while BPS and BPF urine levels have been associated with the prevalence of obesity in children (Jacobson et al., 2019; Liu et al., 2019). In any case, bisphenol-induced insulin hypersecretion may be one of the altered processes contributing to insulin resistance, which represents a risk factor for both T2D and obesity (Alonso-Magdalena et al., 2006; Corkey, 2012; Erion and Corkey, 2017).

BPS and BPF trigger their rapid actions at concentrations as low as 1 nM. In the presence of 16.7 mM glucose, both 1 nM BPS and BPF increased insulin secretion. However, in the presence of

8.3 mM glucose 1 nM BPS potentiated GSIS, while 1 nM BPF did not affect insulin release. These findings indicate that BPF has a slightly lower potency than BPS, which is manifested by the lack of BPF effect at 1 nM on K_{ATP} channel activity. The difference in potency seems to be small since 10 nM BPF inhibited K_{ATP} channel activity to a similar extent as 1 nM BPS. Remarkably, bisphenol-induced inhibition of K_{ATP} channels was abolished in cells from BERKO mice. BERKO mice β-cells do not express ERβ (Boronat-Belda et al., 2020). Our previous studies demonstrated that 1 nM of E2, DPN, or BPA similarly affected K_{ATP} channel activity (Soriano et al., 2009; Soriano et al., 2012). These data suggest that ERβ activation inhibits K_{ATP} channels and that binding to ERβ may mediate the acute action of bisphenols. It is unlikely that this fast response, reached in only 10 minutes, depends on transcriptional regulation; on the contrary, it most likely relies on extranuclear-initiated pathways involving ERβ. Our findings with PaPE-1 and molecular dynamics as well as the existence of a pool of ERβ outside the nucleus of mouse β-cells (Alonso-Magdalena et al., 2008) support this statement. Designed to selectively trigger extranuclear-initiated pathways, PaPE-1 was obtained after chemical rearrangement of key elements of the original steroid structure of E2 so that its ER binding affinity was considerably reduced (Madak-Erdogan et al., 2016). These modifications were performed by substituting the B-ring of the steroid and methylating the positions 2 and 6 of the A-ring, which prevents the formation of key hydrogen bonds within the ligand binding domain (Madak-Erdogan et al., 2016). Similar methylations are observed in tetramethyl BPF (TMBPF), which had no estrogenic effect as assayed by E-SCREEN and it has been proposed as a safer substitute of BPA (Soto et al., 2017). Here, PaPE-1 inhibited K_{ATP} channels in islet cells from WT but not from BERKO mice, which indicates that PaPE-1 and bisphenols activate a similar pathway.

How can bisphenols trigger a rapid effect at low nanomolar concentrations when their affinity for ERβ is within the micromolar range? It is important to bear in mind that the maximum response to a ligand does not depend exclusively on the receptor affinity. The efficacy of the conformational change needed to initiate the signaling cascade as well as the coupling to other signaling proteins also play key roles in the ligand-receptor response (Colquhoun, 1998). Even though the details of the whole pathway from ERβ activation to K_{ATP} closure is not completely known, it has been shown that 1 nM E2 closes K_{ATP} channels through an extranuclear-initiated pathway that involved ERβ, membrane guanylate cyclase, cGMP formation and protein kinase G activation (Ropero et al., 1999; Soriano et al., 2009). The efficacy of this pathway is extremely high as explained below.

In addition to the control of the β-cell resting membrane potential, K_{ATP} channels determine the electrical resistance of the β cell membrane (Ashcroft, 2005). When K_{ATP} channels are open, the electrical resistance is low, whereas the resistance is high when these channels are closed. The membrane potential follows Ohm's law, being the product of the electrical resistance of the membrane by the current running across it. This means that, when extracellular glucose is high, K_{ATP} channels are mostly closed and membrane resistance is high. Hence, a small change in current will elicit membrane depolarization, potentiation of electrical activity, and insulin secretion (Ashcroft, 2005). Our results suggest that bisphenol-induced K_{ATP} channel inhibition may lead to enough change in current that will culminate with increased insulin secretion at high glucose. A similar phenomenon is observed with the incretin GLP-1, which acts as an effective secretagogue only when glucose concentrations are stimulatory and a high percentage of K_{ATP} channels are already closed (Holz et al., 1993). Therefore, low doses of bisphenols will be mainly effective under conditions of decreased K_{ATP} channel activity, as seen in the

427 postprandial state. Accordingly, we show that bisphenols are effective insulin secretagogues only
428 when glucose levels are high. Considering that these bisphenols are used in food-contact
429 materials, the likelihood that they will trigger postprandial insulin release in humans could be
430 high.

431 Besides their acute effects, longer treatment with bisphenols elicited changes in gene expression
432 and GSIS. As already mentioned, insulin release is a consequence of the electrical activity of
433 pancreatic β-cells, which is determined by the expression of ion channels as well as their
434 biophysical characteristics. Both BPS and BPF decreased the expression of *Cacna1e*, *Kcnma1*
435 and *Scn9a*, which encode essential subunits of $Ca_v2.3$, $K_{Ca}1.1$, and $Na_v1.7$ channels. BPS
436 decreased the expression of all channel subunits analyzed at 1 nM, while its effect was lower at
437 100 nM and 1 µM, which suggests an NMDR relationship. BPF, however, needed higher doses
438 (at least 100 nM) to change channel subunits expression. Therefore, BPS effects on gene
439 expression were 100- and 1000-fold stronger than BPF.

440 Changes in ion channel expression by 1 nM BPA during 48 h enhanced GSIS (Villar-Pazos et
441 al., 2017; Martinez-Pinna et al., 2019). Here, BPS treatment for 48 h increased GSIS at 1 nM and
442 1 µM in the presence of 8.3 mM glucose, but only 1 nM BPS was effective in the presence of
443 16.7 mM glucose. This was surprising and it may indicate the existence of a BPS-triggered
444 mechanism that depends on glucose concentration. A similar effect was described for BPA
445 (Villar-Pazos et al., 2017), in which BPA exposure for 48 h decreased exocytosis at low glucose
446 (5.6 mM) but increased exocytosis at high glucose concentrations (11 mM). While these findings
447 suggest the existence of a crosstalk between BPA and glucose signaling effects on the exocytotic
448 machinery, the existence of such crosstalk is yet to be elucidated. In addition, it remains to be
449 determined whether K_{ATP} channels play a role in the long-term effects of bisphenols on GSIS.

Exposure to BPF enhanced GSIS only at 1 µM, the same concentration at which gene expression occurred. These results emphasize the different potencies observed between BPS and BPF.

Our results in BERKO mice indicate that both BPS and BPF effects on gene expression are mediated by ERβ. BPF acts within the micromolar range, which is compatible with its ERβ affinity (see below). On the other hand, our data also suggest that 1 nM BPS acts through ERβ, which is surprising if we consider that BPS binds to ERβ and activates the classic nuclear-initiated pathway at higher concentrations. In vitro bioassays using the stably transfected HELN-hERβ cell line, which contains a luciferase gene driven by an ERE under the control of hERβ, have clearly demonstrated that BPA, BPS and BPF behaved as full hERβ agonists with potencies in the following order: BPA>BPF>BPS (Molina-Molina et al., 2013). Additionally, whole-cell competitive binding assays using the same cell line showed IC_{50} values of 0.21±0.01 nM (E2), 401±126 nM (BPA), 1452±261 nM (BPF), and 3452±878 nM (BPS) (Molina-Molina et al., 2013). Although our findings with BPF are compatible with this classic model, this does not seem to be the case for BPA and BPS.

We pointed out in the first part of the Discussion that low doses of bisphenols can signal through extranuclear-initiated pathways in β-cells. We showed that, like bisphenols, PaPE-1 is an agonist that uses this extranuclear pathway to decrease K_{ATP} channel activity in an ERβ-dependent manner. Then, it is possible that an extranuclear-initiated pathway may be implied in bisphenols action to explain their effects at nanomolar concentrations.

As already discussed, the efficacy of bisphenol response would depend on the interaction between ERβ and other proteins involved in extranuclear signaling. Molecular dynamics indicated that dimerization may be important and may explain, at least in part, why BPA and BPS are more potent than BPF. Dimerization is a requisite for ER extranuclear signaling

(Razandi et al., 2004; Levin and Hammes, 2016) and its role deserves further research in the case of bisphenols and other xenoestrogens. Extranuclear signaling by nuclear receptors is a complex phenomenon and there are very few data showing the activation of such extranuclear pathways by endocrine-disrupting chemicals, including bisphenols (Marino et al., 2012; Vinas and Watson, 2013; Nadal et al., 2018). ERs acting through this pathway do not directly engage DNA to regulate transcription but induce non-nuclear signaling cascades that may lead to transcriptional regulation. Extranuclear ERs interact with a plethora of signaling proteins associated to the plasma membrane or present in the cytosol, such as G proteins and other receptors and kinases involved in extranuclear-initiated signaling triggered by estrogens (Levin and Hammes, 2016). These interactions may amplify bisphenol response via extranuclear ERβ as it has been shown for adrenergic and cholinergic receptors, which respond to ultralow concentrations of ligand within the femtomolar range (Civciristov et al., 2018). Thus, it is necessary to further study bisphenol-activated extranuclear-initiated ER signaling pathways to better understand the efficacy of the response. This information is urgently needed to develop improved testing methods for extranuclear-initiated effects as well as to fully explain how low doses of estrogenic endocrine-disrupting chemicals affect several biological processes. Nonetheless, as untangling the detailed molecular mechanisms underlying EDC effects may be a long process, elucidation of such mechanisms should not be a requirement to create public health policies on an urgent matter (e.g. the impact of EDCs on metabolic disorders).

5. Conclusions

Both short- and long-term exposure to BPS and BPF increase glucose-induced insulin release, which is a risk factor for T2D. The short-term effects is likely due to the inhibition of K_{ATP}

496 channels, while the long-term effect seems to be more complex and may include the regulation
497 of voltage-gated Ca^{2+}, Na^{+} and K^{+} channels. As K_{ATP} channel activity, gene expression of ion
498 channel, and insulin release are endpoints relatively easy to be measured, we propose they should
499 be considered key characteristics (La Merrill et al., 2020) to assess the potential hazards of
500 bisphenols.
501 In line with previous work with ERβ agonists and BPA, our findings with BERKO mice and
502 PaPE-1 suggest that bisphenols act as ERβ agonists and activate an extranuclear-initiated
503 pathway.
504 ERβ affinity for BPA and BPS cannot easily explain the biological effects described in the
505 present work and in previous reports. Our data with acute exposure indicate that efficacy may be
506 more important than affinity to explain bisphenol effects at low doses. More experimental data
507 on dimerization and interaction of ERβ with other signaling molecules in its vicinity are needed
508 to fully understand effects at low doses of bisphenols, especially on gene transcription. In any
509 case, our data support that these bisphenols are not a safe alternative to BPA.

Journal Pre-proof

Journal Pre-proof

Figure Legends

Figure 1. BPS and BPF increase glucose-stimulated insulin secretion in mouse islets. **(A-D)** Insulin secretion was measured at 2.8, 8.3 and 16.7 mM glucose in islets from C57BL/6J mice treated *ex vivo* with vehicle (control; black circles and white bars), 1 nM BPS (green circles and light grey bars) or BPF (yellow circles and dark grey bars), or 1 µM BPS (green circles and dark grey bars) or BPF (yellow circles and dark grey bars). **(A and B)** After 2 h of recovery, treatments (vehicle, BPS or BPF) were added to each glucose solution so that the islets remained under treatment during the whole experiment. **(C and D)** Islets were treated *ex vivo* with vehicle BPS or BPF for 48 h, and then, glucose-stimulated insulin secretion was performed in the absence of treatments. Insulin release was measured by ELISA. Data are shown as means ± SEM of six independent islet preparations isolated on three different days: *p≤0.05, **p≤0.01, ***p≤0.001 vs 2.8 mM; $^{\#}$p≤0.05, $^{\#\#}$p≤0.01, $^{\#\#\#}$p≤0.001 comparisons indicated by bars (one-way ANOVA); $^{\&}$p≤0.05 (Student's t-test).

Figure 2. BPS, BPF and PaPE-1 inhibit K_{ATP} channel activity in mouse pancreatic β-cells. **(A)** Representative recordings of K_{ATP} channel activity in β-cells isolated from wild-type (WT) (black traces) or BERKO (red traces) mice in control condition (0 mM glucose; vehicle; left column), in 1 nM BPS (middle column) and in 11 mM glucose (right). Channel openings are represented by downward deflections, reflecting inward currents due to the high K^+ content of the pipette. The abolition of K_{ATP} activity and generation of action currents at 11 mM glucose was used as a positive control of pancreatic β-cell identity (right column). **(B-G)** Quantification of the K_{ATP} channel activity in β-cells isolated from wild-type (WT) **(B, D and F)** or BERKO **(C, E and G)** mice treated *in vitro* with vehicle (black or white circles and white bars), 1 nM BPS (**B and C**; green circles and light grey bars), 10 nM BPF (**D and E**; yellow circles and dark grey bars) or 1 µM PaPE-1 (**F and G**; blue circles and dark grey bars). The effect of three bisphenols was measured after 7±1 min of acute application. Data are represented as a percentage of activity with respect to resting conditions (0 mM Glucose). Experiments were carried out at 32-34ºC. Data are shown as means ± SEM of the number of cells recorded in WT (n=7-9 cells) and BERKO (n=7-9 cells) mice. These cells were isolated from three mice on three different days. *p≤0.05 vs control (Student's paired t-test).

Figure 3. BPA, BPS, BPF and PaPE-1 reduce *Cacna1e*, *Kcnma1*, *Kcnip* and *Scn9a* expression in mouse islets. mRNA expression of *Cacna1e* **(A-D)**, *Kcnma1* **(E-H),** *Kcnip* **(I-L)** and *Scn9a* **(M-P)** was measured in islets from C57BL/6J mice treated *ex vivo* with vehicle (control; black circles and white bars), BPA **(A, E, I and M**; red circles and light grey bars**),** BPS **(B, F, J and N**; green circles and light grey bars**)**, or BPF **(C, G, K and O**; yellow circles and light grey bars**)** or PaPE-1 **(D, H, L and P**; blue circles and light grey bars**)** at 1, 100 and 1000 nM for 48 h. mRNA expression was measured by qRT-PCR and normalized to the housekeeping gene *Hprt1*, and is shown as fold vs. mean of the controls. Data are shown as means ± SEM of

four to twenty-nine independent samples from up to twenty-nine islets preparations isolated on at least three different days: *p≤0.05, **p≤0.01, ***p≤0.001 (ANOVA one way).

Figure 4. Doses of 1 nM BPS and 1 µM BPF reduce whole-cell Ca^{2+} currents via ERβ in *β-cells*. (**A, B, G, H)** Representative recordings of whole-cell Ca^{2+} currents in response to depolarizing voltage pulses (-60 to +70 mv from a holding potential of -70 mV, 50 ms duration) in isolated *β-cells* from wild type (WT, **A and G**) or BERKO (**B and H**) mice upon treatment with vehicle (left black traces), 1 nM BPS (**A and B**) and 1 µM BPF (**G and H**) (right red traces). **(C-D and I-J)** Average relationship between Ca^{2+} current density (Ca^{2+} currents in pA normalized to the cell capacitance in pF) and the voltage of the pulses in wild-type (WT, **E and I**) and BERKO (**D and J**) control cells (black circles) and cells treated with 1 nM BPS (green circles) and 1 µM BPF (yellow circles). **(E-F and K-L)** Average normalized values of current density evoked at 0 mV obtained from the I–V relationship shown in WT mice **(E and K)** and the BERKO littermates **(F and L)** at three different concentrations of each compound (1 nM, 100 nM and 1 µM). The effect of BPS and BPF were measured after 48 h of incubation. Data are shown as means ± SEM of the number of cells recorded in WT (n=10-21 cells) and BERKO (n=7-23cells) mice. These cells were isolated from twelve (six for BPS and six for BPF) mice on at least three different days: *p≤0.05 vs control (one-way ANOVA).

Figure 5. BPS, and BPF, reduce *Cacna1e*, *Kcnma1* and *Scn9a* expression in islets from wild type but not from BERKO mice. mRNA expression of *Cacna1e* **(A and D)**, *Kcnma1* **(B and E)** and *Scn9a* **(C and F)** in islets isolated from wild-type **(A, B and C)** or BERKO **(D, E and F)** mice treated *ex vivo* with vehicle (control; black circles and white bars), 1 nM BPS (green circles and light grey bars), or 1 µM BPF (yellow circles and dark grey bars) for 48 h. mRNA expression was measured by qRT-PCR and normalized to the housekeeping gene *Hprt1,* and is shown as fold vs mean of the controls. Data are shown as means ± SEM of four to eight independent islet preparations isolated on at least three different days: *p≤0.05, **p≤0.01, ***p≤0.001 (ANOVA one way).

Figure 6. Molecular Dynamics. Analysis of trajectories, MM/PBSA solvation binding energies, and intermolecular interaction energies for the rERβ-ΔH12-LBD dimer from the data generated by MD simulations for 1 µs. **(A)** rERβ-ΔH12-LBD dimer secondary structure and electrostatic surface. The LBD cavity has been cut to show a bound ligand inside the structure. In the following panels, *c1* refers to cavity *1* and *c2* refers to *cavity 2*. **(B)** Frequency distributions of the intermolecular protein interaction energy for the subunits of the rERβ-ΔH12-LBD dimer in the presence of different ligands in each LBD cavity. **(C and D)** trajectories of the ligands (RMSD, Å) initially docked in cavity 1 **(C)** and 2 **(D)** of the LBD. **(E and F)** Frequency distributions of the MM/PBSA solvation binding energy values of each ligand attached to cavity 1 **(E)** and 2 **(F)**. **(G)** Frequency distribution of the number of H-bonds between the solute (protein) and the solvent. A Gaussian curve overlaps discrete data. The legends included within each panel indicate the different ligands analyzed.

Journal Pre-proof

AUTHOR INFORMATION

Corresponding Author

* Angel Nadal, Instituto de Investigación, Desarrollo e Innovación en Biotecnología Sanitaria de Elche (IDiBE), Universitas Miguel Hernández, 03202, Elche, Spain.

E-mail: nadal@umh.es

Credit Author Statement

LM: Conceptualization, Supervision, Investigation, Formal Analysis, Visualization, Writing - Review & Editing **JMP**: Conceptualization, Investigation, Formal Analysis, Visualization, Writing - Review & Editing **MCM**: Investigation, Formal Analysis, Visualization, Writing - Review & Editing **RSdS**: Investigation, Formal Analysis, Writing - Review & Editing **RMMG**: Investigation, Formal Analysis, Writing - Review & Editing **SS**: Investigation, Formal Analysis, Visualization, Writing - Review & Editing **IQ**: Visualization, Resources, Funding Acquisition, Writing - Review & Editing **J-AG**: Resources, Writing - Review & Editing **JAE**: Conceptualization, Investigation, Visualization, Resources, Funding Acquisition, Writing - Review & Editing **AN**: Conceptualization, Supervision, Visualization, Resources, Funding Acquisition, Writing - Original Draft, Project Administration. All authors have given approval to the final version of the manuscript.

Funding Sources

This work was supported by BPU2017-86579-R (AN) and BFU2016-77125-R (IQ) and RTI2018-096724-B-C21 (JAE) supported by FEDER/Ministerio de Ciencia e Innovación-Agencia Estatal de Investigación. PROMETEO/2020/006 (AN), PROMETEO/2016/006 (JAE)

and SEJI/2018/023 (LM) supported by Generalitat Valenciana. J-AG was supported by the Robert A. Welch Foundation (E-0004). CIBERDEM is an initiative of the Instituto de Salud Carlos III.

Acknowledgment

The authors thank Maria Luisa Navarro, Salomé Ramon, and Beatriz Bonmati Botella for their excellent technical assistance. We are grateful to the Cluster of Scientific Computing (http://ccc.umh.es/) of the Universitas Miguel Hernández for providing computing facilities.

References

Acconcia, F., Pallottini, V., Marino, M., 2015. Molecular Mechanisms of Action of BPA. Dose Response 13, 1559325815610582.

Alonso-Magdalena, P., Morimoto, S., Ripoll, C., Fuentes, E., Nadal, A., 2006. The estrogenic effect of bisphenol A disrupts pancreatic beta-cell function in vivo and induces insulin resistance. Environ Health Perspect 114, 106-112.

Alonso-Magdalena, P., Quesada, I., Nadal, A., 2011. Endocrine disruptors in the etiology of type 2 diabetes mellitus. Nat Rev Endocrinol 7, 346-353.

Alonso-Magdalena, P., Ropero, A.B., Carrera, M.P., Cederroth, C.R., Baquie, M., Gauthier, B.R., Nef, S., Stefani, E., Nadal, A., 2008. Pancreatic insulin content regulation by the estrogen receptor ER alpha. PLoS One 3, e2069.

American Diabetes, A., 2018. 2. Classification and Diagnosis of Diabetes: Standards of Medical Care in Diabetes-2018. Diabetes Care 41, S13-S27.

Ascenzi, P., Bocedi, A., Marino, M., 2006. Structure-function relationship of estrogen receptor alpha and beta: impact on human health. Mol Aspects Med 27, 299-402.

Ashcroft, F.M., 2005. ATP-sensitive potassium channelopathies: focus on insulin secretion. J Clin Invest 115, 2047-2058.

Batista, T.M., Alonso-Magdalena, P., Vieira, E., Amaral, M.E., Cederroth, C.R., Nef, S., Quesada, I., Carneiro, E.M., Nadal, A., 2012. Short-term treatment with bisphenol-A leads to metabolic abnormalities in adult male mice. PLoS One 7, e33814.

Beausoleil, C., Emond, C., Cravedi, J.P., Antignac, J.P., Applanat, M., Appenzeller, B.R., Beaudouin, R., Belzunces, L.P., Canivenc-Lavier, M.C., Chevalier, N., Chevrier, C., Elefant, E., Eustache, F., Habert, R., Kolf-Clauw, M., Le Magueresse-Battistoni, B., Mhaouty-Kodja, S., Minier, C., Multigner, L., Schroeder, H., Thonneau, P., Viguie, C., Pouzaud, F., Ormsby, J.N.,

Rousselle, C., Verines-Jouin, L., Pasquier, E., Michel, C., 2018. Regulatory identification of BPA as an endocrine disruptor: Context and methodology. Mol Cell Endocrinol 475, 4-9.
Beydoun, H.A., Khanal, S., Zonderman, A.B., Beydoun, M.A., 2014. Sex differences in the association of urinary bisphenol-A concentration with selected indices of glucose homeostasis among U.S. adults. Ann Epidemiol 24, 90-97.
Biasini, M., Bienert, S., Waterhouse, A., Arnold, K., Studer, G., Schmidt, T., Kiefer, F., Gallo Cassarino, T., Bertoni, M., Bordoli, L., Schwede, T., 2014. SWISS-MODEL: modelling protein tertiary and quaternary structure using evolutionary information. Nucleic Acids Res 42, W252-258.
Boronat-Belda, T., Ferrero, H., Al-Abdulla, R., Quesada, I., Gustafsson, J.A., Nadal, A., Alonso-Magdalena, P., 2020. BISPHENOL-A EXPOSURE DURING PREGNANCY ALTERS PANCREATIC beta-CELL DIVISION AND MASS IN MALE MICE OFFSPRING: A ROLE FOR ERbeta. Food Chem Toxicol, 111681.
Celik, L., Lund, J.D., Schiott, B., 2007. Conformational dynamics of the estrogen receptor alpha: molecular dynamics simulations of the influence of binding site structure on protein dynamics. Biochemistry 46, 1743-1758.
Chen, L., Chen, J., Zhou, G., Wang, Y., Xu, C., Wang, X., 2016. Molecular Dynamics Simulations of the Permeation of Bisphenol A and Pore Formation in a Lipid Membrane. Sci Rep 6, 33399.
Civciristov, S., Ellisdon, A.M., Suderman, R., Pon, C.K., Evans, B.A., Kleifeld, O., Charlton, S.J., Hlavacek, W.S., Canals, M., Halls, M.L., 2018. Preassembled GPCR signaling complexes mediate distinct cellular responses to ultralow ligand concentrations. Sci Signal 11.
Colquhoun, D., 1998. Binding, gating, affinity and efficacy: the interpretation of structure-activity relationships for agonists and of the effects of mutating receptors. Br J Pharmacol 125, 924-947.
Corkey, B.E., 2012. Banting lecture 2011: hyperinsulinemia: cause or consequence? Diabetes 61, 4-13.
Delfosse, V., Grimaldi, M., Pons, J.L., Boulahtouf, A., le Maire, A., Cavailles, V., Labesse, G., Bourguet, W., Balaguer, P., 2012. Structural and mechanistic insights into bisphenols action provide guidelines for risk assessment and discovery of bisphenol A substitutes. Proc Natl Acad Sci U S A 109, 14930-14935.
Delgado, J., Radusky, L.G., Cianferoni, D., Serrano, L., 2019. FoldX 5.0: working with RNA, small molecules and a new graphical interface. Bioinformatics 35, 4168-4169.
Duan, Y., Yao, Y., Wang, B., Han, L., Wang, L., Sun, H., Chen, L., 2018. Association of urinary concentrations of bisphenols with type 2 diabetes mellitus: A case-control study. Environ Pollut 243, 1719-1726.
Encinar, J.A., Fernandez-Ballester, G., Galiano-Ibarra, V., Micol, V., 2015. In silico approach for the discovery of new PPARgamma modulators among plant-derived polyphenols. Drug Des Devel Ther 9, 5877-5895.
Erion, K.A., Corkey, B.E., 2017. Hyperinsulinemia: a Cause of Obesity? Curr Obes Rep 6, 178-186.
Ferguson, M., Lorenzen-Schmidt, I., Pyle, W.G., 2019. Bisphenol S rapidly depresses heart function through estrogen receptor-beta and decreases phospholamban phosphorylation in a sex-dependent manner. Sci Rep 9, 15948.

690 Fratev, F., 2015. Activation helix orientation of the estrogen receptor is mediated by receptor
691 dimerization: evidence from molecular dynamics simulations. Phys Chem Chem Phys 17,
692 13403-13420.
693 Galiano, V., Garcia-Valtanen, P., Micol, V., Encinar, J.A., 2016. Looking for inhibitors of the
694 dengue virus NS5 RNA-dependent RNA-polymerase using a molecular docking approach. Drug
695 Des Devel Ther 10, 3163-3181.
696 Gao, X., Ma, J., Chen, Y., Wang, H.S., 2015. Rapid responses and mechanism of action for low-
697 dose bisphenol S on ex vivo rat hearts and isolated myocytes: evidence of female-specific
698 proarrhythmic effects. Environ Health Perspect 123, 571-578.
699 Gore, A.C., Chappell, V.A., Fenton, S.E., Flaws, J.A., Nadal, A., Prins, G.S., Toppari, J.,
700 Zoeller, R.T., 2015. EDC-2: The Endocrine Society's Second Scientific Statement on Endocrine-
701 Disrupting Chemicals. Endocr Rev 36, E1-E150.
702 Hagobian, T.A., Bird, A., Stanelle, S., Williams, D., Schaffner, A., Phelan, S., 2019. Pilot Study
703 on the Effect of Orally Administered Bisphenol A on Glucose and Insulin Response in Nonobese
704 Adults. J Endocr Soc 3, 643-654.
705 Heldring, N., Pike, A., Andersson, S., Matthews, J., Cheng, G., Hartman, J., Tujague, M., Strom,
706 A., Treuter, E., Warner, M., Gustafsson, J.A., 2007. Estrogen receptors: how do they signal and
707 what are their targets. Physiol Rev 87, 905-931.
708 Hiriart, M., Velasco, M., Larque, C., Diaz-Garcia, C.M., 2014. Metabolic syndrome and ionic
709 channels in pancreatic beta cells. Vitam Horm 95, 87-114.
710 Holz, G.G.t., Kuhtreiber, W.M., Habener, J.F., 1993. Pancreatic beta-cells are rendered glucose-
711 competent by the insulinotropic hormone glucagon-like peptide-1(7-37). Nature 361, 362-365.
712 Jacobson, D.A., Shyng, S.L., 2020. Ion Channels of the Islets in Type 2 Diabetes. J Mol Biol
713 432, 1326-1346.
714 Jacobson, M.H., Woodward, M., Bao, W., Liu, B., Trasande, L., 2019. Urinary Bisphenols and
715 Obesity Prevalence Among U.S. Children and Adolescents. J Endocr Soc 3, 1715-1726.
716 Jereva, D., Fratev, F., Tsakovska, I., Alov, P., Pencheva, T., Pajeva, I., 2017. Molecular
717 dynamics simulation of the human estrogen receptor alpha: contribution to the pharmacophore of
718 the agonists. Mathematics and Computers in Simulation 133, 124-134.
719 Keminer, O., Teigeler, M., Kohler, M., Wenzel, A., Arning, J., Kassner, F., Windshugel, B.,
720 Eilebrecht, E., 2019. A tiered high-throughput screening approach for evaluation of estrogen and
721 androgen receptor modulation by environmentally relevant bisphenol A substitutes. Sci Total
722 Environ, 134743.
723 Kolla, S., Morcos, M., Martin, B., Vandenberg, L.N., 2018. Low dose bisphenol S or ethinyl
724 estradiol exposures during the perinatal period alter female mouse mammary gland development.
725 Reprod Toxicol 78, 50-59.
726 Krege, J.H., Hodgin, J.B., Couse, J.F., Enmark, E., Warner, M., Mahler, J.F., Sar, M., Korach,
727 K.S., Gustafsson, J.A., Smithies, O., 1998. Generation and reproductive phenotypes of mice
728 lacking estrogen receptor beta. Proc Natl Acad Sci U S A 95, 15677-15682.
729 La Merrill, M.A., Vandenberg, L.N., Smith, M.T., Goodson, W., Browne, P., Patisaul, H.B.,
730 Guyton, K.Z., Kortenkamp, A., Cogliano, V.J., Woodruff, T.J., Rieswijk, L., Sone, H., Korach,
731 K.S., Gore, A.C., Zeise, L., Zoeller, R.T., 2020. Consensus on the key characteristics of
732 endocrine-disrupting chemicals as a basis for hazard identification. Nat Rev Endocrinol 16, 45-
733 57.

Lang, I.A., Galloway, T.S., Scarlett, A., Henley, W.E., Depledge, M., Wallace, R.B., Melzer, D., 2008. Association of urinary bisphenol A concentration with medical disorders and laboratory abnormalities in adults. JAMA 300, 1303-1310.

Le Magueresse-Battistoni, B., Multigner, L., Beausoleil, C., Rousselle, C., 2018. Effects of bisphenol A on metabolism and evidences of a mode of action mediated through endocrine disruption. Mol Cell Endocrinol 475, 74-91.

Levin, E.R., Hammes, S.R., 2016. Nuclear receptors outside the nucleus: extranuclear signalling by steroid receptors. Nat Rev Mol Cell Biol 17, 783-797.

Li, Y., Perera, L., Coons, L.A., Burns, K.A., Tyler Ramsey, J., Pelch, K.E., Houtman, R., van Beuningen, R., Teng, C.T., Korach, K.S., 2018. Differential in Vitro Biological Action, Coregulator Interactions, and Molecular Dynamic Analysis of Bisphenol A (BPA), BPAF, and BPS Ligand-ERalpha Complexes. Environ Health Perspect 126, 017012.

Liao, C., Liu, F., Alomirah, H., Loi, V.D., Mohd, M.A., Moon, H.B., Nakata, H., Kannan, K., 2012a. Bisphenol S in urine from the United States and seven Asian countries: occurrence and human exposures. Environ Sci Technol 46, 6860-6866.

Liao, C., Liu, F., Guo, Y., Moon, H.B., Nakata, H., Wu, Q., Kannan, K., 2012b. Occurrence of eight bisphenol analogues in indoor dust from the United States and several Asian countries: implications for human exposure. Environ Sci Technol 46, 9138-9145.

Liu, B., Lehmler, H.J., Sun, Y., Xu, G., Sun, Q., Snetselaar, L.G., Wallace, R.B., Bao, W., 2019. Association of Bisphenol A and Its Substitutes, Bisphenol F and Bisphenol S, with Obesity in United States Children and Adolescents. Diabetes Metab J 43, 59-75.

Madak-Erdogan, Z., Kim, S.H., Gong, P., Zhao, Y.C., Zhang, H., Chambliss, K.L., Carlson, K.E., Mayne, C.G., Shaul, P.W., Korach, K.S., Katzenellenbogen, J.A., Katzenellenbogen, B.S., 2016. Design of pathway preferential estrogens that provide beneficial metabolic and vascular effects without stimulating reproductive tissues. Sci Signal 9, ra53.

Malaise, Y., Lencina, C., Cartier, C., Olier, M., Menard, S., Guzylack-Piriou, L., 2020. Perinatal oral exposure to low doses of bisphenol A, S or F impairs immune functions at intestinal and systemic levels in female offspring mice. Environ Health 19, 93.

Marino, M., Pellegrini, M., La Rosa, P., Acconcia, F., 2012. Susceptibility of estrogen receptor rapid responses to xenoestrogens: Physiological outcomes. Steroids 77, 910-917.

Martinez-Pinna, J., Marroqui, L., Hmadcha, A., Lopez-Beas, J., Soriano, S., Villar-Pazos, S., Alonso-Magdalena, P., Dos Santos, R.S., Quesada, I., Martin, F., Soria, B., Gustafsson, J.A., Nadal, A., 2019. Oestrogen receptor beta mediates the actions of bisphenol-A on ion channel expression in mouse pancreatic beta cells. Diabetologia 62, 1667-1680.

Molina-Molina, J.M., Amaya, E., Grimaldi, M., Saenz, J.M., Real, M., Fernandez, M.F., Balaguer, P., Olea, N., 2013. In vitro study on the agonistic and antagonistic activities of bisphenol-S and other bisphenol-A congeners and derivatives via nuclear receptors. Toxicol Appl Pharmacol 272, 127-136.

Mustieles, V., D'Cruz, S.C., Couderq, S., Rodriguez-Carrillo, A., Fini, J.B., Hofer, T., Steffensen, I.L., Dirven, H., Barouki, R., Olea, N., Fernandez, M.F., David, A., 2020. Bisphenol A and its analogues: A comprehensive review to identify and prioritize effect biomarkers for human biomonitoring. Environ Int 144, 105811.

Nadal, A., Alonso-Magdalena, P., Soriano, S., Quesada, I., Ropero, A.B., 2009. The pancreatic beta-cell as a target of estrogens and xenoestrogens: Implications for blood glucose homeostasis and diabetes. Mol Cell Endocrinol 304, 63-68.

779 Nadal, A., Fuentes, E., Ripoll, C., Villar-Pazos, S., Castellano-Munoz, M., Soriano, S., Martinez-
780 Pinna, J., Quesada, I., Alonso-Magdalena, P., 2018. Extranuclear-initiated estrogenic actions of
781 endocrine disrupting chemicals: Is there toxicology beyond paracelsus? J Steroid Biochem Mol
782 Biol 176, 16-22.
783 Nadal, A., Soria, B., 1997. Glucose metabolism regulates cytosolic Ca2+ in the pancreatic beta-
784 cell by three different mechanisms. Adv Exp Med Biol 426, 235-243.
785 Pike, A.C.W., Brzozowski, A.M., Walton, J., Hubbard, R.E., Thorsell, A.-G., Li, Y.-L.,
786 Gustafsson, J.-Å., Carlquist, M., 2001. Structural Insights into the Mode of Action of a Pure
787 Antiestrogen. Structure 9, 145-153.
788 Quesada, I., Fuentes, E., Viso-Leon, M.C., Soria, B., Ripoll, C., Nadal, A., 2002. Low doses of
789 the endocrine disruptor bisphenol-A and the native hormone 17beta-estradiol rapidly activate
790 transcription factor CREB. FASEB J 16, 1671-1673.
791 Ranciere, F., Botton, J., Slama, R., Lacroix, M.Z., Debrauwer, L., Charles, M.A., Roussel, R.,
792 Balkau, B., Magliano, D.J., Group, D.E.S.I.R.S., 2019. Exposure to Bisphenol A and Bisphenol
793 S and Incident Type 2 Diabetes: A Case-Cohort Study in the French Cohort D.E.S.I.R. Environ
794 Health Perspect 127, 107013.
795 Razandi, M., Pedram, A., Merchenthaler, I., Greene, G.L., Levin, E.R., 2004. Plasma membrane
796 estrogen receptors exist and functions as dimers. Mol Endocrinol 18, 2854-2865.
797 Rochester, J.R., Bolden, A.L., 2015. Bisphenol S and F: A Systematic Review and Comparison
798 of the Hormonal Activity of Bisphenol A Substitutes. Environ Health Perspect 123, 643-650.
799 Ropero, A.B., Alonso-Magdalena, P., Garcia-Garcia, E., Ripoll, C., Fuentes, E., Nadal, A., 2008.
800 Bisphenol-A disruption of the endocrine pancreas and blood glucose homeostasis. Int J Androl
801 31, 194-200.
802 Ropero, A.B., Fuentes, E., Rovira, J.M., Ripoll, C., Soria, B., Nadal, A., 1999. Non-genomic
803 actions of 17beta-oestradiol in mouse pancreatic beta-cells are mediated by a cGMP-dependent
804 protein kinase. J Physiol 521 Pt 2, 397-407.
805 Rorsman, P., Ashcroft, F.M., 2018. Pancreatic beta-Cell Electrical Activity and Insulin
806 Secretion: Of Mice and Men. Physiol Rev 98, 117-214.
807 Ruiz-Torres, V., Losada-Echeberria, M., Herranz-Lopez, M., Barrajon-Catalan, E., Galiano, V.,
808 Micol, V., Encinar, J.A., 2018. New Mammalian Target of Rapamycin (mTOR) Modulators
809 Derived from Natural Product Databases and Marine Extracts by Using Molecular Docking
810 Techniques. Mar Drugs 16.
811 Salentin, S., Schreiber, S., Haupt, V.J., Adasme, M.F., Schroeder, M., 2015. PLIP: fully
812 automated protein-ligand interaction profiler. Nucleic Acids Res 43, W443-447.
813 Santin, I., Dos Santos, R.S., Eizirik, D.L., 2016. Pancreatic Beta Cell Survival and Signaling
814 Pathways: Effects of Type 1 Diabetes-Associated Genetic Variants. Methods Mol Biol 1433, 21-
815 54.
816 Shankar, A., Teppala, S., 2011. Relationship between urinary bisphenol A levels and diabetes
817 mellitus. J Clin Endocrinol Metab 96, 3822-3826.
818 Shtaiwi, A., Adnan, R., Khairuddean, M., Al-Qattan, M., 2018. Molecular dynamics simulation
819 of human estrogen receptor free and bound to morpholine ether benzophenone inhibitor. Theor.
820 Chem. Acc. 137, 10.
821 Smith, C.L., O'Malley, B.W., 2004. Coregulator function: a key to understanding tissue
822 specificity of selective receptor modulators. Endocr Rev 25, 45-71.
823 Soriano, S., Alonso-Magdalena, P., Garcia-Arevalo, M., Novials, A., Muhammed, S.J., Salehi,
824 A., Gustafsson, J.A., Quesada, I., Nadal, A., 2012. Rapid insulinotropic action of low doses of

bisphenol-A on mouse and human islets of Langerhans: role of estrogen receptor beta. PLoS One 7, e31109.
Soriano, S., Ropero, A.B., Alonso-Magdalena, P., Ripoll, C., Quesada, I., Gassner, B., Kuhn, M., Gustafsson, J.A., Nadal, A., 2009. Rapid regulation of K(ATP) channel activity by 17{beta}-estradiol in pancreatic {beta}-cells involves the estrogen receptor {beta} and the atrial natriuretic peptide receptor. Mol Endocrinol 23, 1973-1982.
Soto, A.M., Schaeberle, C., Maier, M.S., Sonnenschein, C., Maffini, M.V., 2017. Evidence of Absence: Estrogenicity Assessment of a New Food-Contact Coating and the Bisphenol Used in Its Synthesis. Environ Sci Technol 51, 1718-1726.
Stahlhut, R.W., Myers, J.P., Taylor, J.A., Nadal, A., Dyer, J.A., Vom Saal, F.S., 2018. Experimental BPA Exposure and Glucose-Stimulated Insulin Response in Adult Men and Women. J Endocr Soc 2, 1173-1187.
Valdeolmillos, M., Nadal, A., Contreras, D., Soria, B., 1992. The relationship between glucose-induced K+ATP channel closure and the rise in [Ca2+]i in single mouse pancreatic beta-cells. J Physiol 455, 173-186.
Vettorazzi, J.F., Ribeiro, R.A., Borck, P.C., Branco, R.C., Soriano, S., Merino, B., Boschero, A.C., Nadal, A., Quesada, I., Carneiro, E.M., 2016. The bile acid TUDCA increases glucose-induced insulin secretion via the cAMP/PKA pathway in pancreatic beta cells. Metabolism 65, 54-63.
Villar-Pazos, S., Martinez-Pinna, J., Castellano-Munoz, M., Alonso-Magdalena, P., Marroqui, L., Quesada, I., Gustafsson, J.A., Nadal, A., 2017. Molecular mechanisms involved in the non-monotonic effect of bisphenol-a on ca2+ entry in mouse pancreatic beta-cells. Sci Rep 7, 11770.
Vinas, R., Watson, C.S., 2013. Bisphenol S disrupts estradiol-induced nongenomic signaling in a rat pituitary cell line: effects on cell functions. Environ Health Perspect 121, 352-358.
Wetherill, Y.B., Akingbemi, B.T., Kanno, J., McLachlan, J.A., Nadal, A., Sonnenschein, C., Watson, C.S., Zoeller, R.T., Belcher, S.M., 2007. In vitro molecular mechanisms of bisphenol A action. Reprod Toxicol 24, 178-198.
Ye, X., Wong, L.Y., Kramer, J., Zhou, X., Jia, T., Calafat, A.M., 2015. Urinary Concentrations of Bisphenol A and Three Other Bisphenols in Convenience Samples of U.S. Adults during 2000-2014. Environ Sci Technol 49, 11834-11839.
Zhang, Z., Hu, Y., Guo, J., Yu, T., Sun, L., Xiao, X., Zhu, D., Nakanishi, T., Hiromori, Y., Li, J., Fan, X., Wan, Y., Cheng, S., Li, J., Guo, X., Hu, J., 2017. Fluorene-9-bisphenol is anti-oestrogenic and may cause adverse pregnancy outcomes in mice. Nat Commun 8, 14585.

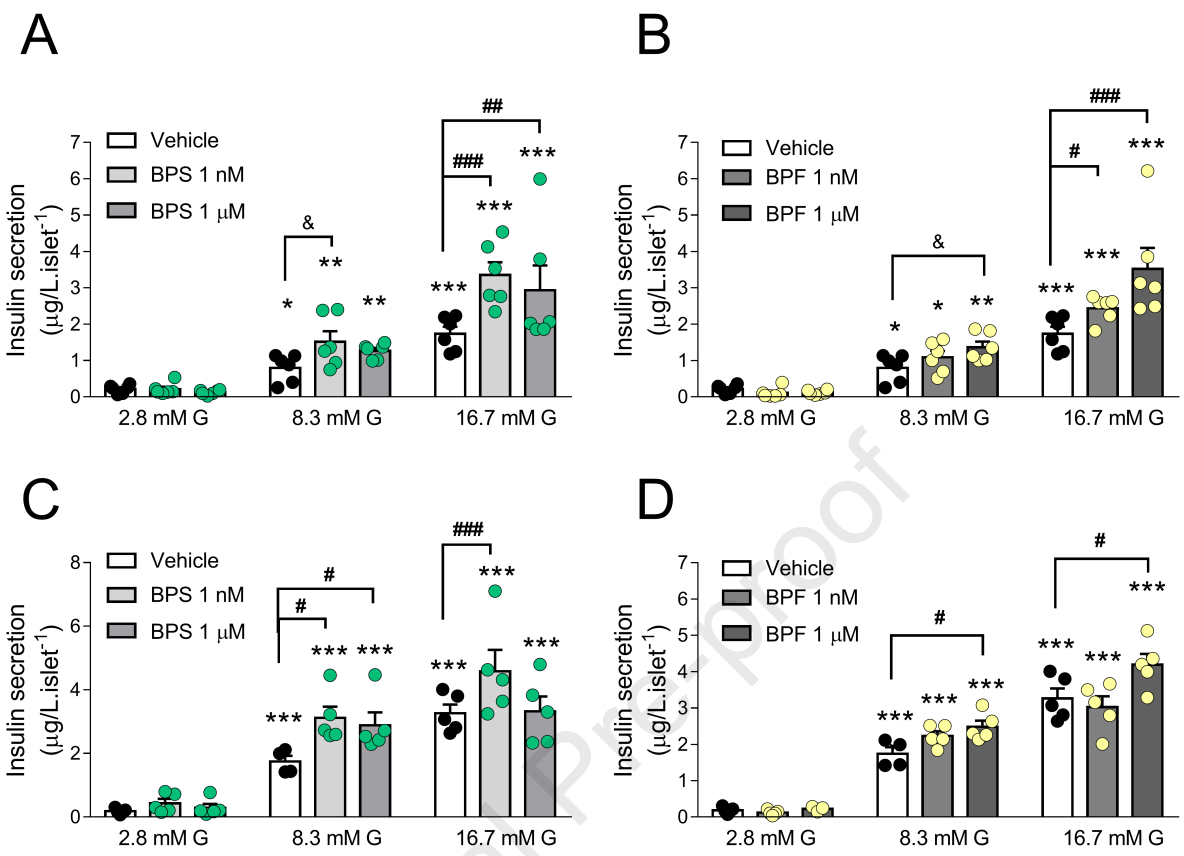

Journal Pre-proof

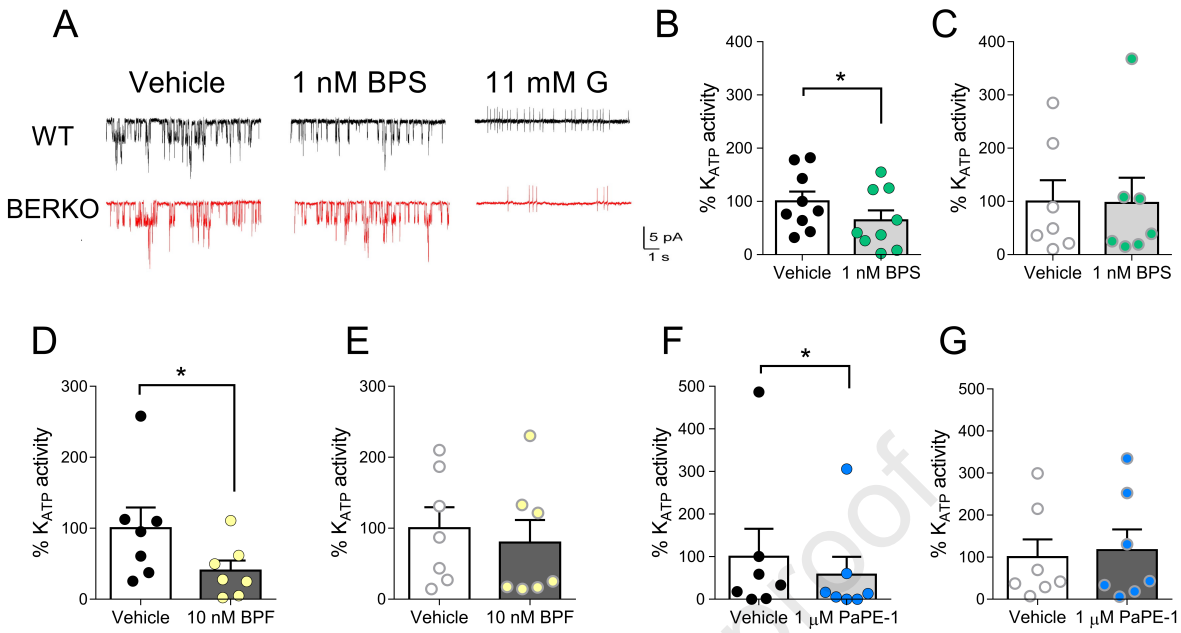

Journal Pre-proof

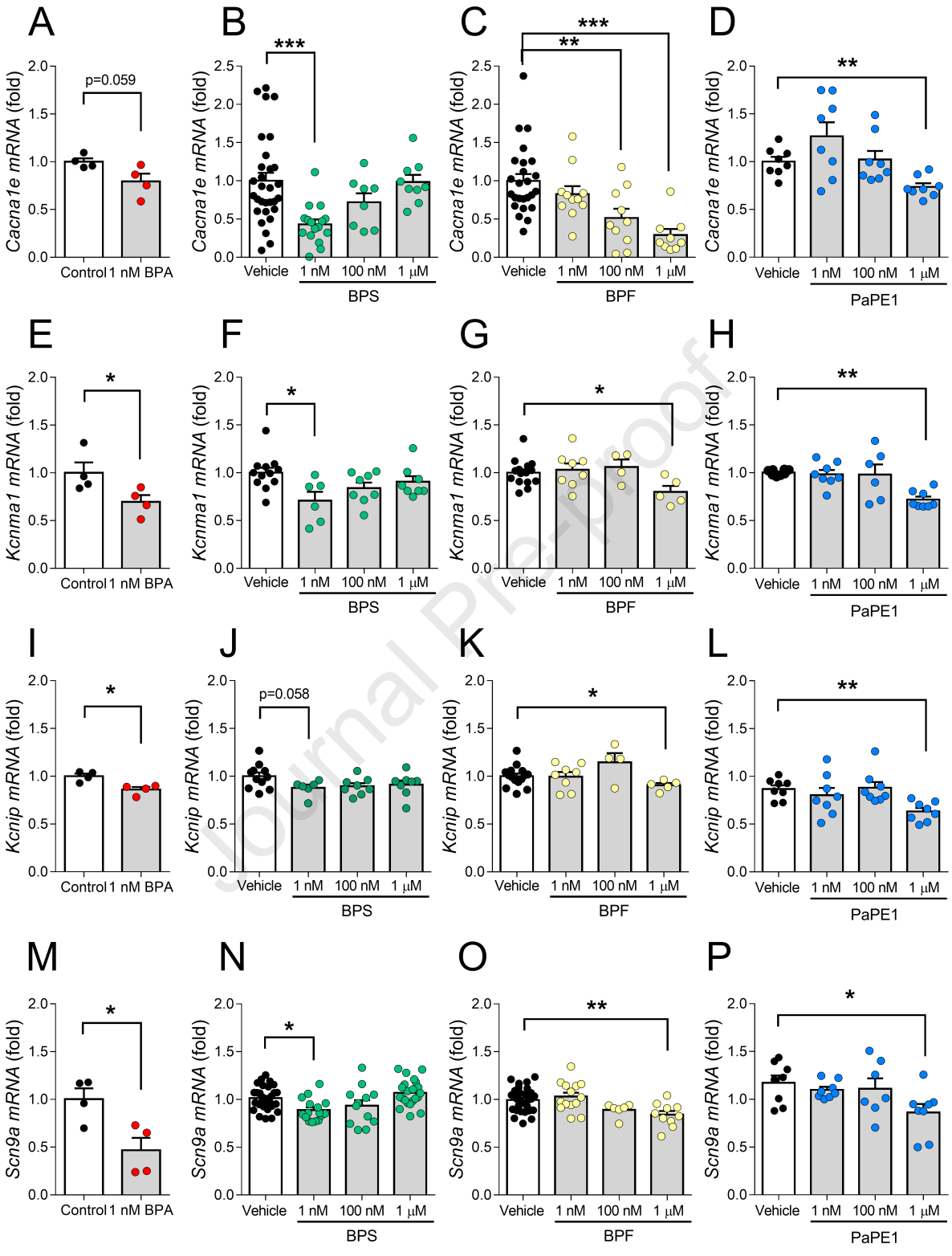

Journal Pre-proof

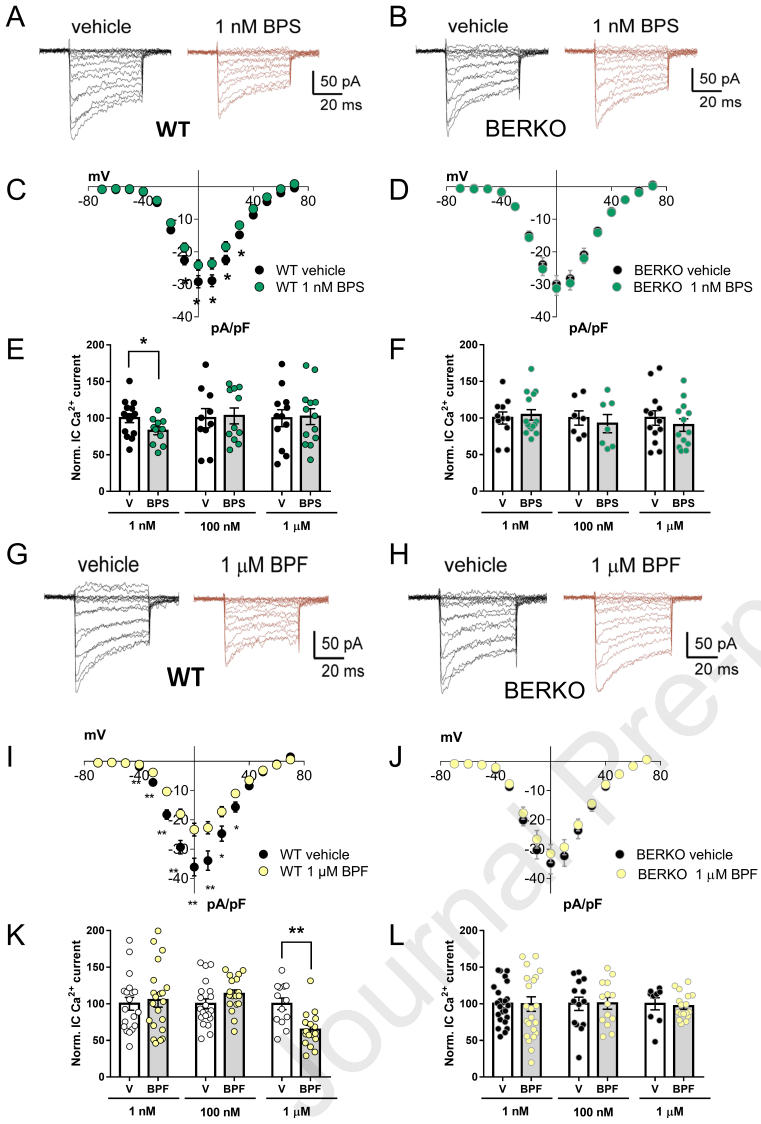

Journal Pre-proof

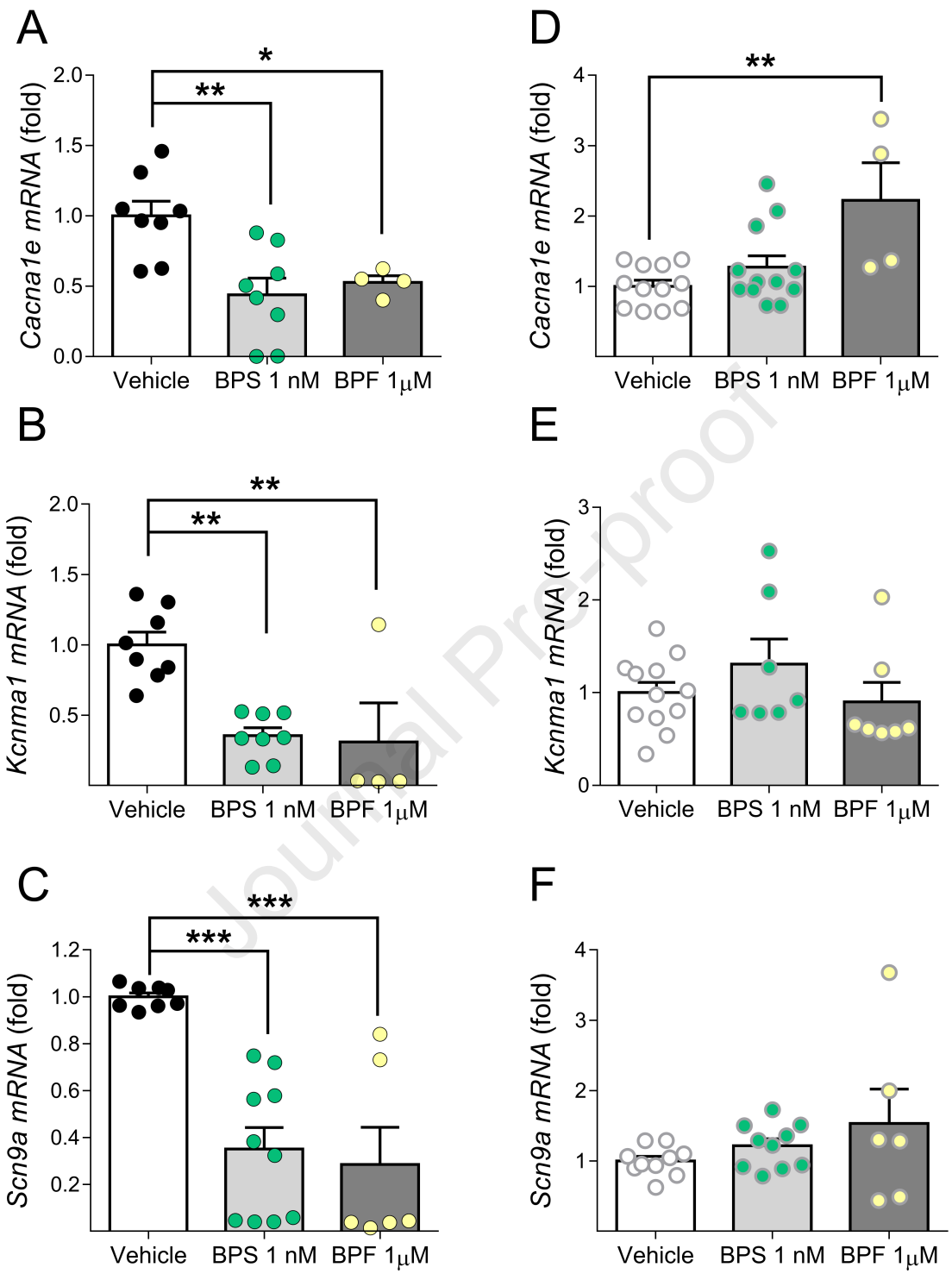

Journal Pre-proof

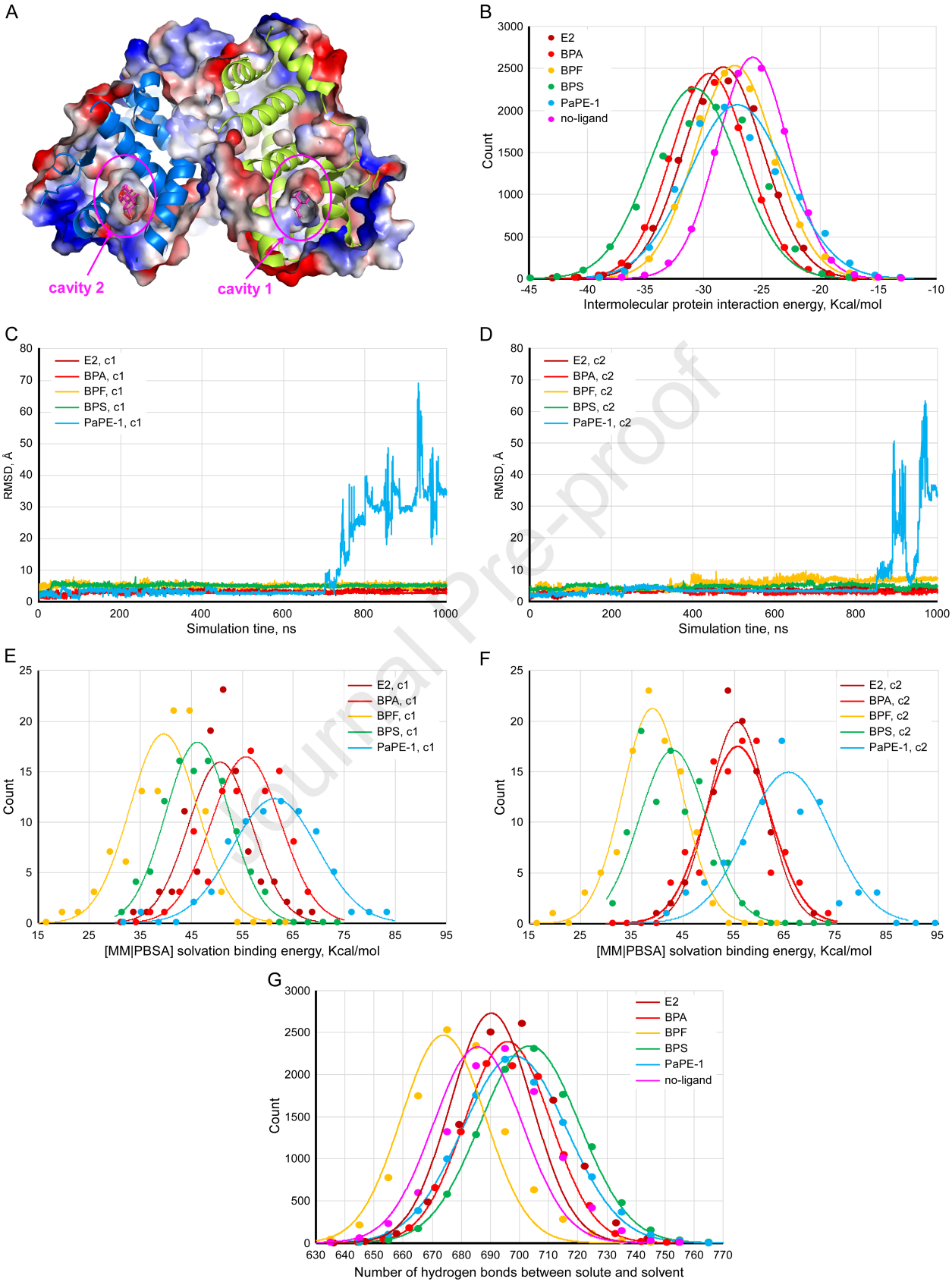

Journal Pre-proof

- Environmental doses of Bisphenol-S and Bisphenol-F enhanced glucose-stimulated insulin secretion, a key characteristic in the control of blood glucose homeostasis.

- These effects seem to be due to changes in activity and gene expression of some ion channels involved in the control of insulin release.

- The potency of Bisphenol-S was significantly higher compared to Bisphenol-F.

- The Estrogen Receptor (ER) β mediated bisphenols effects via an extranuclear-initiated pathway.

- The ERβ extranuclear-initiated pathway may constitute a molecular event whose activation leads to alteration of β-cell function.

Journal Pre-proof

Journal Pre-proof

Declaration of interests

☒ The authors declare that they have no known competing financial interests or personal relationships that could have appeared to influence the work reported in this paper.

☐The authors declare the following financial interests/personal relationships which may be considered as potential competing interests:

Journal Pre-proof